Mass transfer across single bubbles

Kelvin Loh[1], Khoo Boo Cheong[2] and Rob Uittenbogaard[3]

[1] *Singapore-Delft Water Alliance, Department of Civil Engineering, National University of Singapore, Singapore, E-mail: kklloh@nus.edu.sg*
[2] *Singapore-Delft Water Alliance, Department of Mechanical Engineering, National University of Singapore, Singapore, E-mail: mpekbc@nus.edu.sg*
[3] *Deltares & Singapore-Delft Water Alliance, Netherlands, Email: Rob.Uittenbogaard@deltares.nl*

Abstract. Studies done on mass transfer across thin films have established that Hanratty's β (surface divergence) parameter is an important factor determining the mass transfer rate of specie across the gas-water interface. The present work is an attempt to ascertain if the β parameter is a dominant factor governing the scalar transport across the bubble surface as in a bubbly flow. Our work begun with a numerical study used to design the experimental setup for the next stage. By assuming that the empirical models relating β and K_L are still valid, our preliminary results indirectly show that the relation between β and K_L given by Law and Khoo (2002) is still valid for bubble sizes between 2 and 12 mm.
Key Words: bubble, mass transfer, beta parameter

1. Introduction

Numerous studies have established Hanratty's (1991) β parameter (also equivalent to the surface divergence term), as the key kinematic parameter which governs the mass transfer velocity of a dissolved specie across the gas-water interface. However, a majority of the research devoted on mass transfer across bubbles has not systematically established the fundamental factors affecting the value of K_L (the mass transport velocity across the gas-liquid interface). This is due to experimental challenges associated with the continuous movement and fluctuations of the bubble surface. In addition, the concentration of the gasses in the bubble are not constant, as mentioned by Gulliver (2007). The current work attempts to ascertain numerically if the β parameter is still the major factor governing the scalar transport of a specie across the bubble surface. By using the β parameter which is only derived from the fluid velocity gradient near the interface, an empirical model from Law and Khoo (2002) or McCready *et al*. (1986) can be used to obtain the K_L value without the need to solve for the scalar mass transport

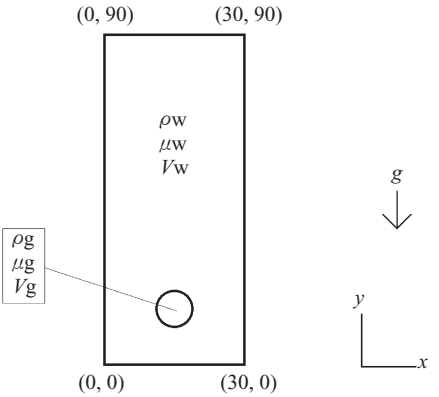

Figure 1 Setup for 12 mm rising bubble problem

equation which saves computational time. Establishing the K_L-β relation is the main objective of our research.

We begin with a single, pure O_2 2D bubble with an initial diameter of 12 mm similar to that found in Krishna and van Baten (1999). The simulations assume a non-contaminated bubble, since, according to the rise velocity and K_L experimental data produced by Alves *et al*. (2004), the simulation time considered is too short for contamination to affect the bubble hydrodynamics. After the relatively large scale hydrodynamics of the single bubble rising (i.e. bubble rise velocity and qualitatively, the general bubble shape) are shown to be accurate by comparing the results with the 2D computational results from Krishna and van Baten (1999), the work proceeds with a series of smaller bubbles ranging from 2 to 6 mm with 1 mm increments. The values obtained for the smaller bubbles are then compared with the experimental results of 3D bubbles from Motarjemi and Jameson (1978). The motivation to simulate a 2D bubble instead of a 3D bubble stems from the high computational cost involved in capturing the gradient of the velocities at the bubble interface for a 3D bubble. Since this is a preliminary study for a future experimental work, the cost involved for a 3D bubble is significant. Figure 1 shows the problem geometry and initial conditions for the case study of the 12 mm bubble, and the smaller diameter bubbles with the coordinates in units of mm.

2. Mathematical Formulation

2.1 Governing Equations

We used the 2D *FLUENT* finite volume code solver to solve the 2D Navier Stokes equations (Eq. 1). The energy equation is not solved since the problem is a

low-speed flow problem and heat transfer was not considered in the problem. The governing equations are

$$\begin{aligned} &\nabla\cdot\vec{U}=0\\ &\partial_t(\rho\vec{U})+\nabla\cdot(\rho\vec{U}\otimes\vec{U})=-\nabla p+\nabla\cdot\underline{\underline{S}}+\rho\vec{g}\\ &\underline{\underline{S}}=\mu(\nabla\vec{U}+(\nabla\vec{U})^T). \end{aligned} \tag{1}$$

where $\vec{U}$ is the mixture fluid velocity vector, ρ is the mixture density, p is the pressure field in the domain, $\underline{\underline{S}}$ is the viscous shear stress tensor, and $\vec{g}$ is the gravitational acceleration vector.

The non-slip and a constant surface tension conditions at the gas-water interface are

$$\begin{aligned} &[\vec{U}]=0\\ &[p\mathrm{I}-\underline{\underline{S}}]\cdot\vec{n}_\Sigma=-\sigma(\vec{n}_\Sigma\nabla\cdot\vec{n}_\Sigma).\\ &\vec{n}_\Sigma=\frac{\nabla f}{|\nabla f|} \end{aligned} \tag{2}$$

where $\vec{n}_\Sigma$ is the unit normal of the bubble interface pointing from gas to water domain, and f is the volume fraction variable used to denote whether the cell is completely filled with water (f=1), gas (f=0), or a mixture of both which is the interface of the bubble (0<f<1).

Youngs' Geo-reconstruct scheme was used to discretize the color function advection equation used (Eq. 5) in the VOF model (Youngs, 1982). Since the simulations times are short (<1 s), assuming a rise velocity of 0.25 m/s, and an initial bubble size of 4 mm, the change in bubble volume is approximately 0. 0024%, hence there are no source/sink terms in the advection equation.

$$\partial_t f+\nabla\cdot(\vec{U}f)=0. \tag{5}$$

The material properties, density ρ, and viscosity μ, in the respective phases are calculated based on a linear interpolation from the volume fraction of the individual phases given by

$$\begin{aligned} &\rho=f\rho_w+(1-f)\rho_g\\ &\mu=f\mu_w+(1-f)\mu_g\,. \end{aligned} \tag{4}$$

2.2 Initial Conditions

The initial conditions for the case of the 12 mm rising bubble are shown in Figure 1. The smaller rising bubble cases have similar case setups except for the different initial bubble diameters. The velocities are initialized at 0 m/s.

Table 1 Boundary conditions for the numerical cases (all numbers are in mm)

Boundary	Rising bubble
(x, 90)	$\frac{\partial U}{\partial y}=\frac{\partial V}{\partial y}=0$
(x, 0)	No-slip
(0, y) and (30, y)	No-slip

Table 2 Material Properties

Material Property	Oxygen	Water
Density (kg/m^3)	1.29	998
Viscosity (Pa.s)	1.79e−5	1e−3

2.3 Boundary Conditions and Material Properties

The boundary conditions used in *FLUENT* for the rising bubble setup (bubble diameters ranging from 2 to 12 mm) are provided in Table 1.

The boundary conditions for the rising bubble cases are applied similar to the setup by Krishna and van Baten (1999). Table 2 shows the material properties used in the simulations.

3. Computational Methodology

3.1 Numerical Methods

The equations are solved in a segregated manner using the SIMPLE scheme proposed by Patankar (1980). The momentum equations were discretized using the second-order upwind scheme. The PRESTO! (Pressure Staggering Option) scheme was used for the pressure interpolation. The Volume-Of-Fluid (VOF) method of Hirt and Nichols (1981) was used to track the interface between the two phases.

A first-order implicit time stepping scheme was used with the Courant number set at 0.95 to ensure temporal resolution as well as solution accuracy.

3.2 Mesh Generation

The mesh generation for the cases were relatively straightforward considering the simplicity of the geometries. They are all structured uniform meshes, except for the adaptive mesh that was used in the 5 mm stationary bubble in a tube. Since the work currently involves purely numerical results, a grid convergence study was performed for validation purposes. This was carried out for the typical 4 mm rising bubble setup. Figure 2 shows the result for the grid convergence study with

Table 3 Mesh size for the different cases

Mesh Size	Rising bubble (2−12 mm)
$\Delta x=\Delta y$ (mm)	0.025−0.05

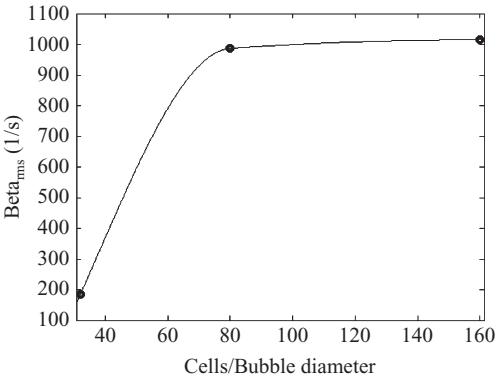

Figure 2 Grid convergence study for 4 mm rising bubble

the β_{rms} value being the deciding quantity. The β_{rms} value is the spatial root-mean-square value for the normal gradient of the velocity normal to the gas-water interface. The finest grid has a cell area of Δx^2＝6.25E－4 mm^2 (160 cells per bubble diameter) and the largest grid having a cell area of 1.5625E-2 mm^2 (32 cells per bubble diameter).

Table 3 shows the grid size used for all the cases.

4. Results and discussion

4.1 Bubble rise velocity

The 12 mm rising bubble case was used as a test case for the *FLUENT* code. The mesh used for the bubble rise velocity cases are of the coarser mesh since the gradient of the velocity at the interface was not needed. Hence, a large simulation time can be performed (approximately 0.5 s). Preliminary results show that the VOF calculations by *FLUENT* using Youngs' Geo-Reconstruct interface reconstruction scheme is an improvement over the simulations via *CFX* by Krishna and van Baten (1999) using CICSAM. Figure 3 shows the velocity magnitude contours with the interface shown at f＝0.5. The shape of the bubble is clearly defined when compared with the snapshots of the simulation done by Krishna and van Baten (1999) (see Figure 4)and the flow structure around the bubble is similar to most rising bubbles with vortices formed downstream of the bubble and a recirculation zone near the vicinity of the bubble. The animation of

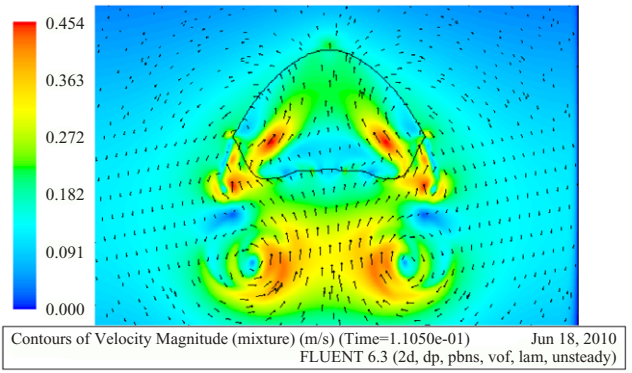

Figure 3 12 mm bubble velocity magnitude contour

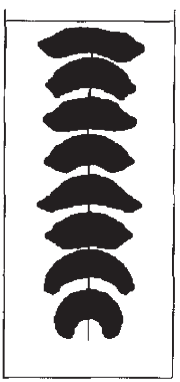

Figure 4 Snapshots of the *CFX* simulations from Krishna and van Baten (1999)

this simulation can be found on *http: //www. youtube. com/watch? V = JDs_ 6jxC7qw*. Figure 5 shows a modified graph from Krishna and van Baten (1999) on the experimental results of the bubble terminal velocity as a function of bubble diameter, together with the computed 2D results from *FLUENT* and *CFX*. It can be seen that the *FLUENT* code gives a prediction which is closer to the experiments than the result obtained from *CFX*. This is most likely due to improved numerical schemes as well as better interface reconstruction schemes available in the newer version of *FLUENT* in 2006, as compared to the numerical schemes implemented in earlier *CFX*. This observation is also confirmed by Ozkan *et al*. (2007) for the rise velocity of a bubble in a narrow channel.

Figure 6 shows the bubble terminal velocities as a function of bubble diameter as calculated from *FLUENT* and compared with the experimental data featuring

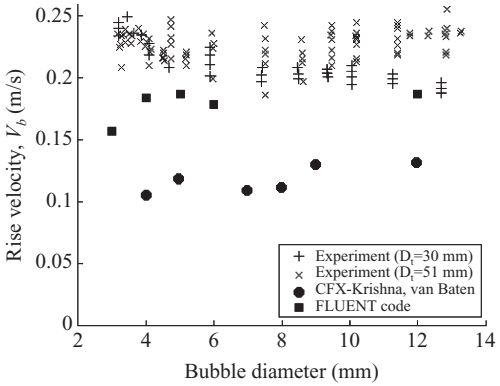

Figure 5 Terminal velocity result for the 12 mm 2D rising bubble compared with CFX in 2D, and experiments with 3D spherical bubbles (D_t is the column diameter of the experimental setup)

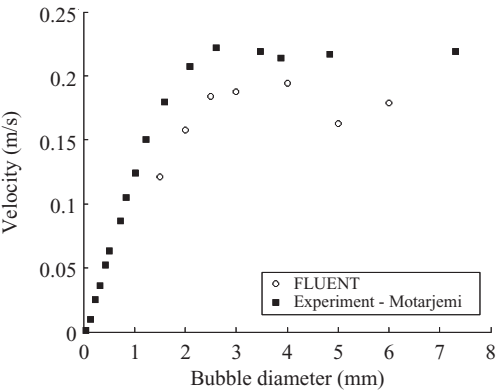

Figure 6 Terminal velocity as a function of bubble diameter

3D spherical bubbles by Motarjemi and Jameson (1978). As can be seen from the two curves, the code shows a similar trend for the 2 mm bubble to the 6 mm bubble. Smaller bubble sizes were not tested considering the computational costs involved. Another reason for not testing the smaller bubble sizes is due to the fact that for bubbles between 0.04 mm to 0.3 mm, the less expensive Stokes' equation can be used to predict the bubble rise velocity within reasonable accuracy. Figure 6 does not show the data point for the 12 mm bubble because Motarjemi and Jameson (1978) did not have any data points for bubbles larger than 6 mm. The results from Figure 5 and Figure 6 also show that the computational results consistently underpredict the actual terminal velocity of the bubbles for both the

FLUENT and *CFX* code. This is due to the 2D assumption of a 3D spherical bubble. This observation is also confirmed by Dijkhuizen *et al*. (2005). They observed that the 2D VOF model consistently has a higher drag coefficient than the 3D front tracking model employed by them, resulting in the 2D bubbles having lower terminal velocities.

4.2 Mass transfer velocity

We apply empirically the mass transport velocity relation proposed by Law and Khoo (2002) based on the spatially averaged β_{rms} value (Xu *et al*. 2008) defined as

$$K_L = \sqrt{0.05 \cdot D \cdot \beta_{rms}}$$
$$\beta_{rms} = \sqrt{\frac{\int_0^L \beta^2 ds}{\int_0^L ds}} \tag{3}$$
$$\beta = \frac{\partial w}{\partial z} = -\left(\frac{\partial u}{\partial x} + \frac{\partial v}{\partial y}\right)$$

where K_L is the mass transport velocity of the specie related empirically to β_{rms}, D is the diffusion coefficient of the specie in water, and w (normal), u (tangential), and v (tangential), the velocity components of the fluid with respect to the interface, and dz (normal), dx (tangential), and dy (tangential), the spatial derivatives with respect to the interface.

For the calculation of β_{rms}, the interface normal were obtained from the VOF curvature data at the interface used to calculate the surface tension force source term in the momentum equation (see Brackbill *et al*. 1992). In *FLUENT*, the velocity gradients are in the Cartesian co-ordinates, hence, a transformation matrix based on the curvature data was used to transform the gradients into the interface normal reference frame. A User-Defined-Function (UDF) was written in C to calculate the value of the β_{rms} at each timestep.

For the mass transfer velocity calculations of the 12 mm rising bubble, the β_{rms} value of the bubble reaches a steady state value at 902 s^{-1}, which when using Law and Khoo's empirical relation, Eq. 3, gives a value for the K_L of 0.031 cm/s based on D = 2.1E-9 m^2/s for pure O_2 in water at a temperature of 298.15 K. Figure 7 and Figure 8 show the β_{rms}, and K_L for the 12 mm rising bubble case as a function of distance travelled by the bubble normalized by the bubble diameter, respectively.

The K_L values used for comparison are based on Higbie's (1935) penetration theory, and Calderbank-Moo Young (1961). Higbie's penetration theory predicts a K_L of 0.0236 cm/s based on the time it takes for the bubble to travel one bubble diameter. As for Calderbank-Moo Young's prediction, the K_L predicted was 0.041

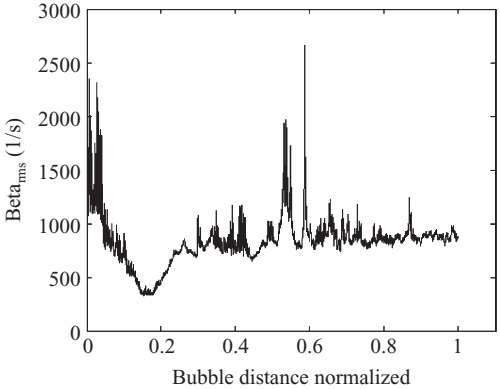

Figure 7 β_{rms} as a function of normalized distance (12 mm)

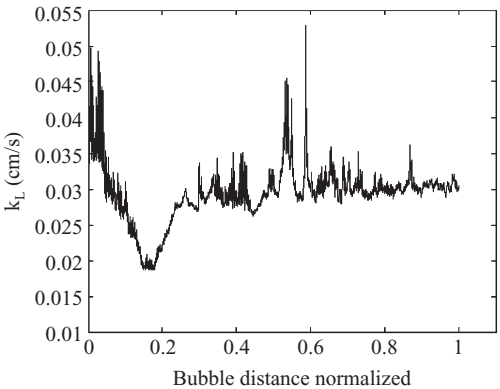

Figure 8 K_L from empirical model of Law & Khoo (2002) as a function of normalized distance (12 mm)

cm/s. Since the value obtained from *FLUENT* and Law and Khoo's relation gives 0.031 cm/s, the value is within the range predicted by these two theories. The slight drop in the β_{rms} could possibly be due to effects of the start of the "flapping" motion of the bubble. Based on Xu *et al*. (2008), this transient effect should be ignored since the spatial averaged β_{rms} should remain constant and this is shown with the steady state values of the β_{rms} given in Figure 7. Also, the total simulation time is for that single bubble to travel a bubble diameter. This is a relatively short simulation time as the mesh used is the finer mesh and the computational time to compute up to 0.4 s would be too prohibitive for a preliminary study.

For the smaller rising bubble diameters ranging from 2 to 6 mm, the comparison is made with the experimental results from Motarjemi (1978). Figure 9 shows the mass transfer velocity calculated using the relation of Law and Khoo

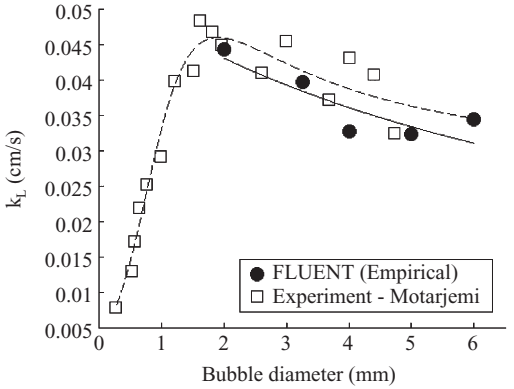

Figure 9 K_L as a function of bubble diameter (obtained from Law & Khoo relation)

(2002) and the β_{rms} parameter from *FLUENT* as a function of the bubble diameter. The dashed and solid lines are curve fits for the experimental and computational results, respectively. It can be seen that yet again, the trend shows a good comparison with experimental results, but due to the 2D approximation of the bubbles as well as the employment of numerical viscosity for stability, the computational results for the β_{rms} quantity which is dependent on the velocity field are under predicted.

5. Conclusions

The preliminary results of the numerical simulations show that Hanratty's β parameter is still an important parameter for the mass transfer velocity (K_L) of a specie across a rising single bubble. For rising bubbles which have diameters between 2 to 12 mm, it is found that the empirical relation given by Law and Khoo (2002) relating K_L to β_{rms} can be applied with good concurrency with experiments. As such, using similar models which computes for β_{rms}, one can then predict the mass transfer without having to calculate for the mass transfer equation across the deformable bubble surface.

Future work that needs to be done will include the mass transport equation with the proper treatment of jump conditions across the bubble interface to compare directly with the experimental results obtained using PIV measurements.

References

Alves, S.S., Orvalho, S.P., and Vasconcelos, J.M.T. (2005), Effect of bubble contamination on rise velocity and mass transfer, *Chemical Engineering Science, 60*, 1-9.

Brackbill, J.U., Kothe, D.B., and Zemach, C. (1992), A Continuum Method for Modeling

Surface Tension, *J. Comp. Phys., 100*, 335-354.

Calderbank, P.H. and Moo-Young, M.B. (1961), The continuous phase heat and mass-transfer properties of dispersions, *Chemical Engineering Science, 16*, 39-54.

Dijkhuizen, W., van den Hengel, E.I.V., Deen, N.G.. van Sint Annaland, M., Kuipers, J.A. M. (2005), Numerical investigation of closures for interface forces acting on single air-bubbles in water using Volume of Fluid and Front Tracking models, *Chemical Engineering Science, 60*, 6169-6175.

Gulliver, J.S. (2007), *Introduction to Chemical Transport in the Environment* (Book), 1st ed., 196 pp., Cambridge University Press, New York, USA.

Hanratty, T.J. (1991), Effect of Gas Flow on Physical Absorption (Proceeding), *Proceeding of the 2nd International Symposium on Gas Transfer at Water Surfaces.* (Eds. S.C. Wilhelms & J.S. Gulliver), American Society of Civil Engineers, 10-33.

Higbie, R. (1935), *A.I.Ch.E. Journal, 31*, 365.

Hirt, C.W. and Nichols B.D. (1981), Volume of Fluid (VOF) Method for the Dynamics of Free Boundaries (Journal), *J. Comp. Phys.*, *39*, 201-225.

Krishna, R. and van Baten, J.M. (1999), Rise Characteristics of Gas Bubbles in a 2D Rectangular Column: VOF Simulations VS Experiments (Journal), *Int. Comm. Heat Mass Transfer, 26(7)*, 965-974.

Law, C. and Khoo, B.C. (2002), Transport across a turbulent gas-liquid interface (Journal), *A.I.Ch.E. Journal, 48(9),* 1856-1868.

McCready, M.J., Vassiliadou, E., and Hanratty, T.J. (1986), Computer simulation of turbulent mass transfer at a mobile interface, *A.I.Ch.E. Journal, 32(7)*, 1108-1115.

Motarjemi, M. and Jameson, G.J. (1978), Mass Transfer from Very Small Bubbles – The Optimum Bubble Size for Aeration (Journal), *Chemical Engineering Science, 33*, 1415-1423.

Ozkan, F., Worner, M., Wenka, A., and Soyhan, H.S. (2007), Critical evaluation of CFD codes for interfacial simulation of bubble-train flow in a narrow channel (Journal), *International Journal for Numerical Methods in Fluids, 55*, 537-564.

Patankar, S.V. (1980), *Numerical Heat Transfer and Fluid Flow* (Book), 1st ed., 126 pp., Hemisphere Publishing Corporation, Washington, DC, USA.

Xu, Z.F., Khoo, B.C., and Wijeysundera, N.E. (2008), Mass transfer across the falling film: Simulations and experiments (Journal), *Chemical Engineering Science, 63*, 2559-2575.

Youngs, D.L. (1982), Time-Dependent Multi-Material Flow with Large Fluid Distortion, *Numerical Methods for Fluid Dynamics.* (Eds. K.W. Morton and M.J. Baines), Academic Press, New York, USA.